ISSN 2176-5480

ELECTRIC MOTOR INTERFERENCE LINKAGE FEM VALIDATION AND DESIGN FACTOR DETERMINATION BASED ON THE ASSEMBLY AND MATERIAL PROPERTIES DISTRIBUTIONS

Rafael Beck, rafaelb@weg.net
Matheus André Campregher, matheusc@weg.net
Research and Technological Innovation Department – R&TI
WEG Electric Equipments S.A.
Waldemar Grubba Avenue, 3000 – PO. Box 420
Zip code: 89256-900, Jaraguá do Sul, Santa Catarina, Brazil
Fone: +55 47 32764803 / Fax: +55 47 32764931

Edison da Rosa, edison.rosa@ufsc.br
Mechanical Engineering Department
Federal University of Santa Catarina – PO. Box 476
Zip code: 88040-900, Florianópolis, Santa Catarina, Brazil
Fone/Fax: +55 48 37219899

Abstract. *This paper presents a methodology for validation of a numeric model for an interference linkage assembly between the stator and the frame of a conventional electric motor by means of strain experimentally obtained during the insertion process of the stator into the frame by strain gages attached on the frame critical points. Each simulation cycle necessary to the validation process corresponds to an iteration and the several simulation parameters tested in one iteration are tabulated, including, beyond the numeric versus experimental error, the processing time to achieve the solution using a specific computational platform. This tabulation can be used as a guide for similar numeric simulations. Once validated, the model is used for improvement purposes applied to the conceptual frame design in the manner that the minimum safety factor value in the critical region of the frame is equal or bigger than the calculated design factor. The design factor takes into account data as the reliability level attributed to the design, the resistance dispersion for the material used in the frame manufacture and the stresses dispersion in the critical region of the frame, this one due to different interference linkage assembly tolerances descendants from the production line. In this analysis, both the strength and the stress probabilistic distributions are considered to be normal distribution and the population failure probability is corrected for the finite number of samples used. This procedure is applied in a smaller frame size than the previous one, from the same product line. The data show that the dispersion of the generated stresses in this frame is smaller and follows the also smaller dispersion of the interference linkage assembly. This, on the other hand, is due to the higher stiffness of this frame. This shows that the design factor obtained for the frame with bigger size can be adopted with safety for the other frames which have successively smaller sizes from the same product line, so that, minimizing costs with tests, instrumentation and analysis time.*

Keywords*: Validation, finite element, strain gage, design factor, distribution.*

1. INTRODUCTION

The validation process of theoretical models is extremely important for the industry and has gain evidence due to the growing global concurrence. Although it demands time, money and big effort from the engineer, when it is concluded, the validation represents competitive gains. Models correctly validated allow confidence on its response, and so, allowing that one goes beyond the previous limits concerning product optimization. As an example, if there is confidence in the stress response of a specific critical point in a structure model, there is more comfort to propose even mass reduction in this structure, seeking for material costs reduction. Besides, it is possible to propose geometric modifications in order to achieve high stiffness-mass relation, if this is the case. Also, a validated model for a specific component subjected to specific boundary conditions can be used for other components from the same family, but with different sizes, since they are subjected to the same boundary conditions. This is the case of the electric motors product line studied in this paper. The proposed numerical model is validated for the biggest frame size from this product line, namely, the IEC 132 frame. This frame is the most critical because it has the lowest stiffness between all the others, which are smaller ones. Once validated, the model is expanded and used for one of the smaller frames.

Referring to the elaboration of theoretical models, certainly the numerical models deserve merit, especially the ones created by the finite element method (FEM). This is an extremely spread method and its progress was outstanding in the 1970 decade. Today, almost all big company makes use of FEM as an analysis tool.

Another very useful tool and at the same time little used in the validation process and development as a whole is the statistics, or being more specific to the solid mechanics, the structural reliability methodology. Despite of the theory is well established, the authors have the opinion that its use is confined to the academy and, excluding in leading companies like the aerospace one, very little companies use this theory as routine in their developments. Therefore,

ISSN 2176-5480

inside the industry in general, this is an extremely fertile field which must be explored. Note at this point, that the deterministic design usually used day to day in the industry allows limited gains, even when the representative model has been validated. Herewith, it is mandatorily caution and the use of higher safety factors, because the deterministic method doesn't take into account subjects like variation in the component production process, which also produces geometric variations; the material mechanical properties variations; and, variations in the solicitations applied in the component in service. That is, for the application of the structural reliability theory, it is primordial the deep knowledge of the process, the material and the solicitations involved.

2. PROBLEM DESCRIPTION

The electric motors product line target in this paper is derived from another existing line and is destined to a new application, in which the space for the motor installation is extremely restricted. This obligates the motor be installed without the terminal box usually used to promote the cables connections. Instead, just one cover with a cable gland is used to guide the cables toward the electric motor exterior. The use of this cover-cable gland system creates the problem of cables wrinkled because of the low space inside the motor for the cables appropriated curvature, without compromising the safety during assembly and operation. This enforces a machining in the frame, liberating more space for the cables and allowing the appropriate accommodation of them. This is done in a frame region called here the hoop. As the quantity of material removed is considerable, one question arises: Will we have rupture problem in the frame hoop region when it is subjected to the stator insertion? The linkage between the stator and the frame is by interference and one knows that the frames of the existing line don't present this type of problem during the insertion process. In view of this, the analysis was focused only in the tooled hoop behavior, as this is the unique difference in this new electric motors product line. Fig. 1 shows the difference between the standard, or existing frame (a), and the proposed frame (b), in which the hoop is machined.

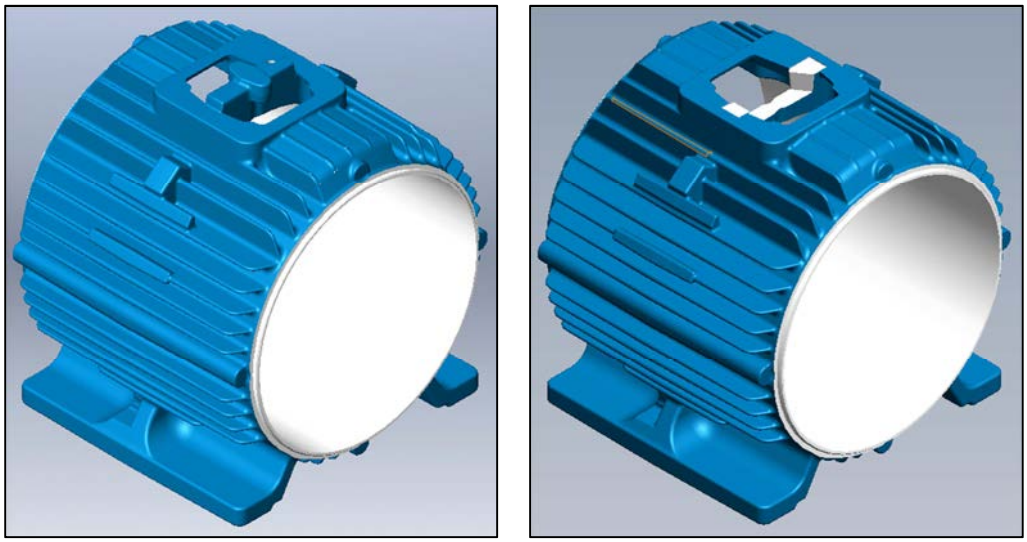

(a) (b)

Figure 1. (a) Standard frame and (b) proposed frame, with machined hoop.

3. EXPERIMENTAL PROCEDURE

To answer the previous question with safety, it was decided to treat the problem in a statistical way, preparing some frames and stators samples, submitting them to the insertion process of the stator into the frame, measuring the resulting strains in the hoop and calculating the corresponding stresses. For this work, it was used the 132 and 112 frame sizes, in agreement with the IEC standard. These frames are the biggest ones for this product line, so it is expected to be the critical ones. Due to economic reasons, it were used only five stator samples and five frame samples for each one of the frame sizes cited. The inner diameters of the frame samples were measured in three different heights by a coordinated measuring machine which has a 0.001 mm precision. The same was done for the stator samples outer diameters. This procedure allows one to know the mean interference between the formed stator/frame pairs. The first criterion to form the pairs was the higher interference. So, the frame with lower inner diameter formed pair with the stator with higher outer diameter, allowing the highest stresses generation. The other pairs were formed in a random way, as it happens in the production line. Table 1 presents the inner frames diameters and outer stators diameters measurement results for both the frame sizes, and likewise, the corresponding interferences. It is also shown the interferences mean values, its standard deviations and dispersion coefficients.

ISSN 2176-5480

Table 1. Frame inner diameters, stator outer diameters, corresponding interferences, mean interference, standard deviations and dispersion coefficients.

IEC 132 Frame/Stator			IEC 112 Frame/Stator		
Frame [mm]	Stator [mm]	Interference [mm]	Frame [mm]	Stator [mm]	Interference [mm]
219.9148	220.0563	0.1415	181.9312	182.0580	0.1268
219.9652	220.0556	0.0904	181.9433	182.0431	0.0998
219.9820	220.0433	0.0613	181.9683	182.0499	0.0816
220.0042	220.0461	0.0419	181.9684	182.0499	0.0815
220.0170	220.0399	0.0229	181.9687	182.0378	0.0690
Mean interference [mm]		0.0716	Mean interference [mm]		0.0917
Standard Deviation [mm]		0.0464	Standard Deviation [mm]		0.0224
Dispersion Coefficient		0.6476	Dispersion Coefficient		0.2446

In order to measure the resulting stresses in the hoop during the insertion process, it were used unidirectional strain gages, positioning them in the critical points and aligning them according to principal stresses directions. The critical points in the hoop and the maximum principal directions were previously obtained by a finite element simulation, however, still not validated. Note that the validation process doesn't alter, in this case, the critical points in the hoop neither the principal stresses direction. It only corrects the values of the resulting stresses. Figure 2 shows one of the frames with the hoop instrumented with three strain gages, called: e1 strain gage placed centrally in the hoop top; e2 strain gage placed laterally in the hoop, next to the hole; and e3, strain gage placed also laterally in the hoop, but next to the its central curvature.

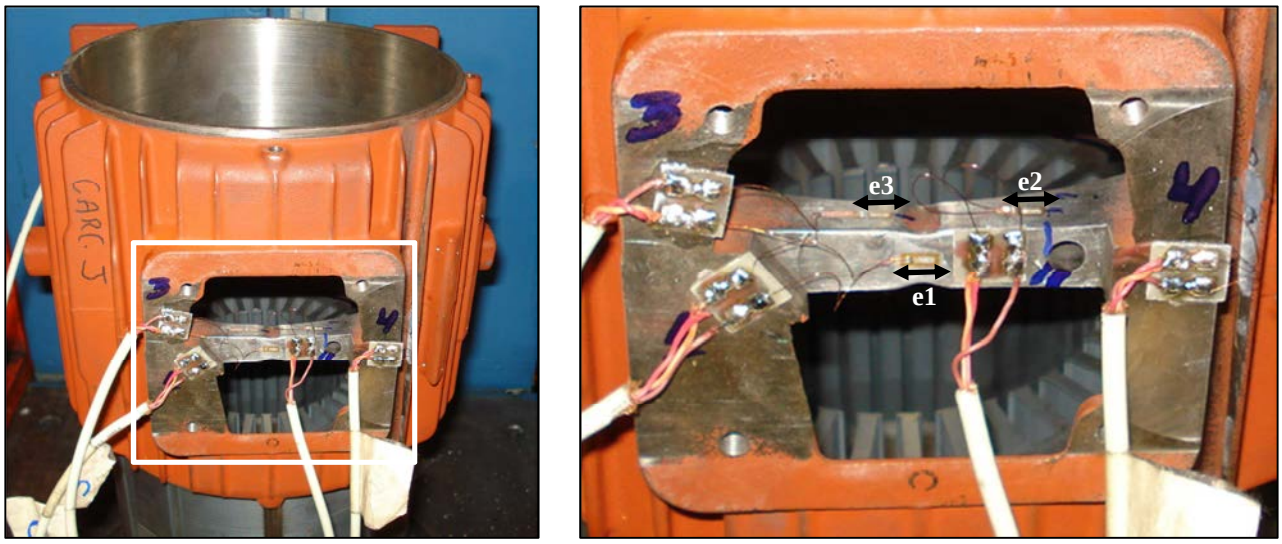

(a) (b)

Figure 2. (a) Instrumented frame region and (b) zoom of this region showing the strain gages.

It is important to have the materials involved in the analysis well characterized. In this study, it is pointed out especially the FC-200 gray cast iron behavior, which is used in the frames production. This material, despite of being brittle, presents extremely non-linear behavior up to its rupture. This behavior starts at about 0.05 % of strain and it is even more evident for higher strain values. In this work, it was obtained extremely high strain values in the hoop, so, the corresponding stress values needed to be estimated by an interpolation over the material experimental stress-strain curve, as shown in Fig. 3 for the 132 stator/frame pair with the highest interference. In the figure, one can see that as the strain becomes higher, it becomes also higher the difference between the linear stresses, estimated using the material elastic modulus and the non-linear stresses, estimated by interpolation over the material experimental stress-strain curve The extreme case happened for the strain gage e1, in which the difference between the linear and non-linear stress value achieved 228 %.

ISSN 2176-5480

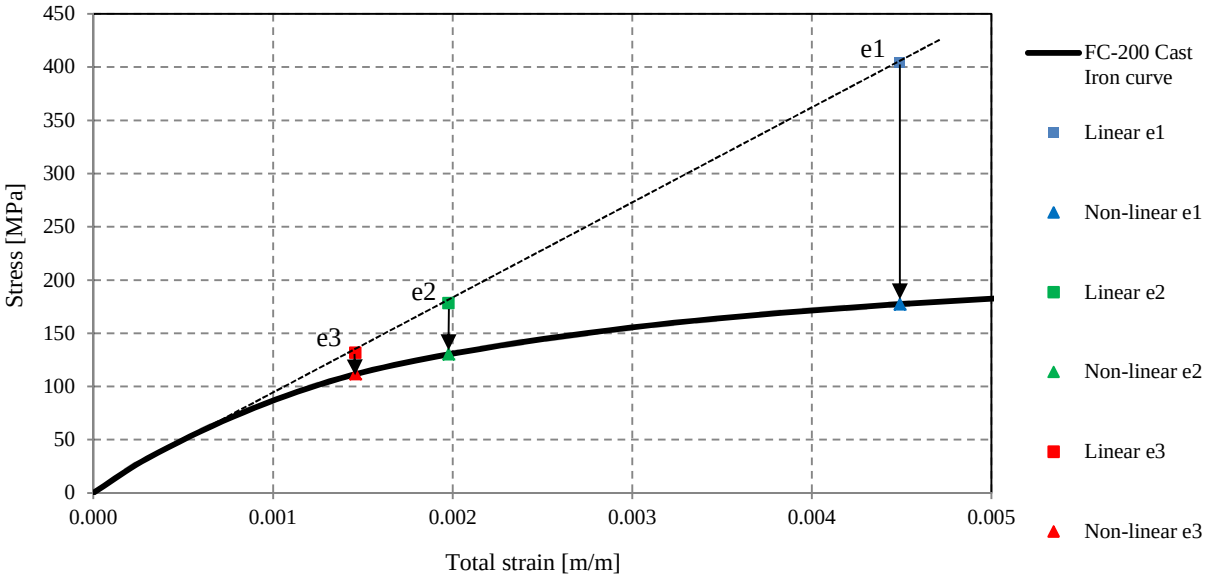

Figure 3. Difference between linear and non-linear stress values.

Another important factor which is characteristic of the interference linkage problem is the stress peaks generated during the insertion process. These are caused by the interference linkage amongst the finishing aspect of the frame tooled surface which is frequently rugged, and due to the fact that the stator is formed by several laminated plates each one with thickness of 0.6 mm successively juxtaposed and grouped by means of metallic clasps. This type of assembly results necessary in plates misalignment, that is, the plates are eccentric with respect to each other. The analysis of all results shown that the maximum difference between a peak stress value and the corresponding stabilized stress value, that is, after the end of the insertion process, is 1.5. This value was called dynamics amplification factor and was used as a multiplier for the stress values in the hoop obtained via MEF, as in this simulation it was considered the par stator/frame already assembled with the corresponding interference. Making a dynamic simulation taking into account the frame inner diameter tooling errors, the rugged originated by this tooling, geometric errors from the stator and more, the misalignment of the stator plates, would be extremely complex and onerous and it is out from the scope of this work.

4. NUMERIC MODEL VALIDATION

4.1. Finite element model

For validation, a finite element model of the IEC 132 frame was used. In this model, the maximum interference between stator-frame was applied. So, it was modeled the stator-frame presented in the first line of Tab. 1, with interference of 0.1415 mm. The other interference cases of Tab. 1 were used for the design factor calculations. The choice for the assembly with the highest interference is due to the fact that the higher the strain measured by the strain gage, the higher the confidence in the measured result, because there is less influence of the tooling errors in the measurement. In fact, the contact region between both the components, stator and frame, was treated as a perfect cylinder, which doesn't represent the reality. For example, graphically the coordinate measuring machine shows the frame inner diameter as an ellipse, which is rotated as it progress through the frame length. This behavior occurs with more or less intensity in all the frames. The stator presents a behavior more stable and more closed to a perfect cylinder in its whole length, even being formed by laminated plates. For the interference calculation, it was used the mean interference value of three measurements in three different heights through the frame and the stator axial lengths, being these positions coincident after the assembly of the two components. As previously attested, representing the geometric errors in the CAD model or even in the CAE model is possible, but is onerous and would demand that the measurements of the both components diameters were made in a much more number of heights through the components axial lengths to make possible the geometry mapping for both components, for each one of the sample assemblies. Again, this process is out from this work scope.

Some modifications in relation to the real components geometry were necessary to minimize the simulation costs. These modifications don't produce great influence in the results and are more outstanding in the stator. In this component, the slots were simply suppressed, remaining just the yoke region. It is considered that this simplification doesn't reduce the component stiffness because the slots are not interconnected. In the other hand, it was considered a two pole motor stator, which has bigger yoke and so, higher stiffness, compared to the other motor polarities. In addition, it was considered the biggest stator length of this product line, promoting deformation in a longer extension of

ISSN 2176-5480

the frame. Several lines were drawn in the CAD model in its inner diameter in order to test different boundary conditions during the validation process. For the frame, the simplifications were limited in the elimination of drilled holes, without influence in the frame stiffness. The interference between the stator and the frame was created in the CAD model. This was done modeling the components with the mean diameters obtained by the coordinate measuring machine, that is, the frame was modeled with its measured mean inner diameter and the stator with its measured mean outer diameter. Figure 4 shows the complete FEM and a detail from the hoop region in top view.

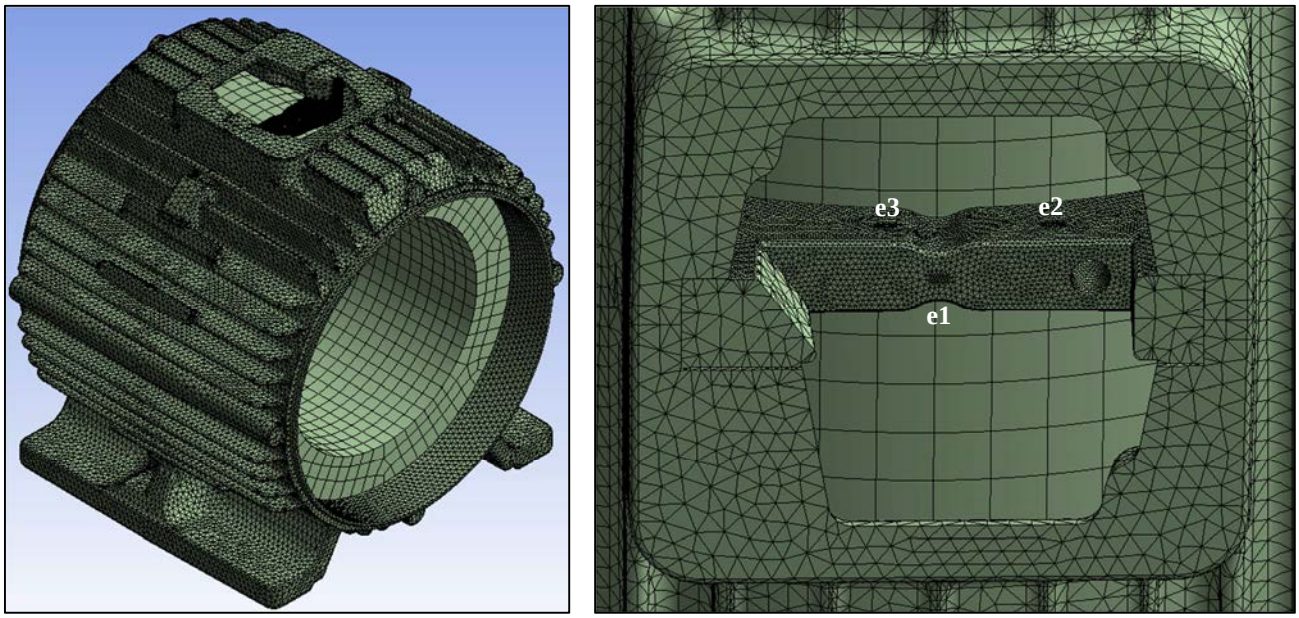

(a) (b)

Figure 4. (a) Complete finite element model and (b) detail from the hoop region with strain gages.

Special attention was given to the strain gages modeling. The localization of each strain gage was defined in previous FEM simulations, choosing critical stressed regions. Once defined these regions, all the strain gages were attached on the frame respecting them. In the CAD, the strain gages were represented by small rectangles, with identical dimensions as the used strain gage grids, according to the supplier catalog. In this case, it were used unidirectional strain gages with grid length x width of 3.18 x 1.52 mm. Inside the grid area, it was evaluated the mean value of the maximum principal stress in the grid direction of all the elements present in the area. These were the stress values tabulated in Tab. 2 and used for the theoretical *versus* experimental error calculations.

During the whole validation process, the mesh parameters were kept the same. In the frame were used second order tetrahedral solid elements. In its body, a finite element global size of 4 mm was adopted. In the frame hoop, were used a 1 mm finite element global size and a refinement guarantee a 0.5 mm finite element global size in the strain gages places. In the stator were used hexahedron solid elements with global size of 10 mm. The choice of these values for the global element sizes came from the balance between mesh quality and processing costs. For all the simulations it was kept the Jacobian ratio equal to 1 for at least 99 % of the elements compounding the frame, which is in fact the component of interest for stress calculation. This indicates that the majority of the elements didn't present significant distortions and so, resulting in lower mapping errors between the CAD and CAE models.

4.2. Material models

The stator core is produced in 1006 steel and the frame in FC-200 gray cast iron. These two materials have a very distinct behavior and must follow distinct material models. The steel has a linear behavior conducted by its elastic modulus. The cast iron behavior is non-linear since about 0.05% of total strain and it is necessary the adoption of a plasticity model to represent that behavior. As cycle loads are not of interested, just the monotonic one, a multilinear isotropic hardening was chosen. This model is represented by Fig. 5, where the equivalent plastic strain is incrementally determined. In this model, the experimental data are supplied in a multilinear table form, where the first point defines the elastic modulus E, and the others, the various tangent elastoplastic modulus, $E_T's$ as in the figure.

ISSN 2176-5480

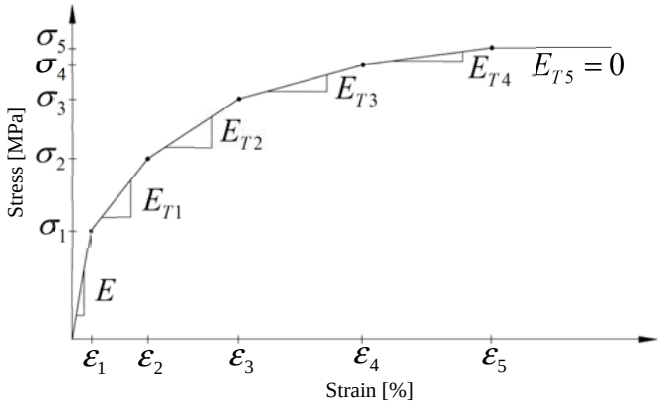

Figure 5. Multilinear isotropic hardening model.

The adopted properties can be seen in Tab. 2. Note that for the cast iron, the finite element code was supplied also with the experimental curve as the one shown in Fig. 3. Besides, both the material were considered to be isotropic.

Table 2. Mechanical properties for FC-200 cast iron and ABNT 1006 steel.

	FC-200 Cast Iron	ABNT 1006 Steel
Elastic modulus, E [GPa]	111.2	211
Poisson coefficient, ν	0.24	0.30
Yield stress, S_e [MPa]	-	220
Tensile ultimate stress, S_{rt} [MPa]	200	420
Compressive ultimate stress, S_{rc} [MPa]	600	-

4.3. Validation discussion

The complete description of all the boundary conditions and the other validation parameters are tabulated in Tab. 3, for the IEC 132 motor with the maximum interference from table I. The achieved elapsed time considers an i7 core, 3.4 GHz processor, 8 GB RAM computational platform.

Table 3. FEM results validation summary for the IEC 132 assembly with the highest inference.

Iteraction	Contact Type	Contact Settings	Boundary Conditions	Simulated Stresses [MPa]			Measured Stresses [MPa]			Error [%]			Elapsed Time [s]	Comments
				e1	e2	e3	e1	e2	e3	e1	e2	e3		
1	Frictional	NFC = 0.2	CSSIDAF	115.5	92.2	75.8				-34.8	-29.1	-32.0	24712	SPC
2	Rough	NFC = NA	CSSIDAF	83.7	71.9	53.6				-52.8	-44.7	-51.9	12190	SPC
3	Frictional	NFC = 0.1	CSSIDAF	121.5	96.6	80.1				-31.4	-25.7	-28.2	29141	SPC
4	Frictional	NFC = 0.1	CSSIDAF	127.5	102.2	84.1				.28.0	-21.4	-24.6	19479	STC
5	Frictional	NFC = 0.01	CSSIDAF	132.7	106.2	88.8	177.2	130.1	111.5	-25.1	-18.4	-20.4	28412	STC
6	Frictional	NFC = 0.001	CSSIDAF	133.2	106.6	89.3				.24.8	-18.1	-19.9	14283	STC
7 (2)	Frictional	NFC = 0.001	CSSIDAF	133.4	106.7	89.4				.24.7	-18.0	-19.8	15922	STC
8	Frictionless	NFC = 0	SIDF /FAVF	163.2	130.5	109.3				-7.9	0.3	-2	3862	STC/HC7
9	Frictionless	NFC = 0	SIDF /FAVF	162.2	129.4	108.6				-8.5	-0.5	-2.6	3912	STC/HC9
→10	Frictionless	NFC = 0	SIDF /FAVF	167.3	134.1	112.3				-5.6	3.1	0.7	3843	STC/HC22

Notes:
(1) Normal stiffness = 0.1 for all the iteractions. Because it reduces the number of iteractions to solution.
(2) Offset = 0.07075 mm. In the other iteractions the interference was insert via CAD model.
(3) Large deflection = Off for all the iteractons.

Legend:
NFC = **N**ormal **f**riction **c**oefficient.
NA = **N**ot **a**pplied. In this case the normal frictional coefficient approaches theoretically infinite.
CSSIDAF = **C**ylindrical **s**upport in the **s**tator **i**nner **d**iameter and **a**xial direction **f**ixed / Frame free.
SIDF = **S**tator **i**nner **d**iameter totally **f**ixed.
FAVF = **F**rame **a**xial and **v**ertical **d**irections **f**ixed.
SPC = **S**tator **p**artially **c**ylindrical.
STC = **S**tator **t**otally **c**ylindrical.

ISSN 2176-5480

HC 7/9/22 = **H**ardening **c**urve **7**%, **9**% e **22**% stiffer than the standardized one.
⟶ = Converged iteraction.

It is important to observe that after the FEM validation, new frames were proposed and simulated using it. However, without modeling the strain gages, once this is only necessary and useful for validation purposes. To evaluate the safety factor in the proposed frames hoops and compare with the determined design factor, the maximum and minimum principal stresses from all the elements nodes compounding the hoop were extracted and the respective safety factors were calculated by the Coulomb-Mohr theory. The criterion for approval was that the safety factor in any hoop point must be higher or at least equal to the determined design factor for the analyzed frame.

5. DESIGN FACTOR DETERMINATION

The design safety factor, or simply design factor, is a statistical safety factor which indicates how safe is a component, given the stress and strength conditions. In fact, the stress and the strength are random variables that follow some given distribution. In this paper, it was considerate that both follows the normal distribution. Once known the solicitation and resistance means and dispersion coefficients, it is possible to calculate the corresponding design factor for the desired confidence level. The equations development for the design factor calculation is described bellow, with the aid of the capacity bound variable. The capacity bound variable, M, is given by the difference between the component mechanical strength, R, and the solicitation on this component, S. Applying the expected value operator, $E[\blacksquare]$, the expected value of the capacity bound variable is given by the difference between the resistance and solicitation expected values,

$$E[M] = E[R] - E[S] \,. \tag{1}$$

The variance σ^2 from the capacity bound will be equal to the sum of the stress and strength variances,

$$\sigma_M{}^2 = \sigma_R{}^2 + \sigma_S{}^2 \,. \tag{2}$$

Now, any distribution can be transformed into a new distribution Z by means of a change of variables. In the case of the capacity bound distribution, the change from the M variable to the new Z variable is given by,

$$z = \frac{m-\mu_M}{\sigma_M} \,, \tag{3}$$

where μ_M is the mean value of the capacity bound and m are the individual values.
Substituting equations (1) and (2) in equation (3), results in,

$$z = \frac{\mu_S-\mu_R}{\sqrt{\sigma_R{}^2+\sigma_S{}^2}} \,. \tag{4}$$

Appyling the square,

$$z^2 = \frac{\mu_R{}^2+\mu_S{}^2-2\mu_R\mu_S}{\sigma_R{}^2+\sigma_S{}^2} \,. \tag{5}$$

The dispersion coefficient V for a distribution is the quotient between its standard deviation σ and its mean μ. For the resistance and solicitation one has, respectively,

$$V_R = \frac{\sigma_R}{\mu_R} \quad \text{and} \quad V_S = \frac{\sigma_S}{\mu_S} \,. \tag{6}$$

Dividing the numerator and denominator in equation (5) by $\mu_S{}^2$ comes,

$$z^2 = \frac{\mu_R{}^2/\mu_S{}^2+1-2\mu_R/\mu_S}{\sigma_R{}^2/\mu_S{}^2+\sigma_S{}^2/\mu_S{}^2} \,. \tag{7}$$

Multiplying and dividing the term $\sigma_R{}^2/\mu_S{}^2$ by $\mu_R{}^2$ and recognizing the equations (6) in the resulting equation,

$$z^2 = \frac{(\mu_R/\mu_S)^2+1-2(\mu_R/\mu_S)}{V_R{}^2(\mu_R/\mu_S)^2+V_S{}^2} \,. \tag{8}$$

Defining the design factor n as,

ISSN 2176-5480

$$n = \frac{\mu_R}{\mu_S} , \tag{9}$$

Equation (8) becomes,

$$z^2 = \frac{n^2+1-2n}{n^2{V_R}^2+{V_S}^2} . \tag{10}$$

Developing equation (10),

$$n^2\left(1 - z^2{V_R}^2\right) - 2n + \left(1 - z^2{V_S}^2\right) = 0 . \tag{11}$$

Calling the term $\left(1 - z^2{V_R}^2\right)$ by δ_R and $\left(1 - z^2{V_S}^2\right)$ by δ_S,

$$n^2\delta_R - 2n + \delta_S = 0 . \tag{12}$$

Equation (12) is a second degree equation and has so two roots given by,

$$n = \frac{2\pm\sqrt{4-4\delta_R\delta_S}}{2\delta_R} . \tag{13}$$

or,

$$n = \frac{1}{\delta_R}\left[1 \pm \sqrt{1 - \delta_R\delta_S}\right] . \tag{14}$$

For safety reasons, one takes the highest design factor given by,

$$n = \frac{1}{\delta_R}\left[1 + \sqrt{1 - \delta_R\delta_S}\right] . \tag{15}$$

The solicitation in the hoop is defined by the stresses in the hoop, which are resulting by the different interferences between stator and frame. For the 132 IEC frame, the experimental results from all the cases in Tab. 1 shown that the highest dispersion in the stress values was observed in the e1 strain gage, placed on center of the top of the hoop. In this strain gage the mean stress value was $\mu_{e1} = 81.52$ MPa and the standard deviation was $\sigma_{e1} = 53.58$ MPa. Equations (6) leads to $V_{e1} = 65.73$ % for the stress dispersion coefficient in the e1 strain gage. This value was adopted as the solicitation dispersion coefficient for the 132 frame, that is,

$$V_S(132) = 65.73\% . \tag{16}$$

The component strength is defined by the FC-200 cas iron ultimate strength, which has mean value of $\mu_{Srt} = 200$ MPa. The observed standard deviation is $\sigma_{Srt} = 26.13$ MPa. Then, the resulting dispersion coefficient is $V_{Srt} = 13.06$ %. This value is true for all the frames from this line of products, since all of then are melt in the same foundry using the same material. Therefore,

$$V_R = 13.06\% . \tag{17}$$

The reliability level, *C*, adopted for the hoop design was 99 %, resulting in $z = 2.326$, considering the normal distrubution for solicitation and resistance. This is true for a infinite number of samples (population). For $N = 5$ samples (number of samples used) this value is corrected and becomes $z_5 = 2.7$ (Kececioglu and Lamarre, 1978).

Using the values from equations (16) and (17) and the z value, δ_S and δ_R are calculated. Using their values in equation (15), results the design factor $n = 3.08$ for the 132 frame, that is,

$$n(132) \cong 3.1 . \tag{18}$$

For the 112 IEC frame the process is the same. The higher dispersion was also observed in the e1 strain gage, placed on the top of the hoop, in its center. In this strain gage, the mean stress value was $\mu_{e1} = 56.84$ MPa and the standard deviation was $\sigma_{e1} = 26.94$ MPa. Herewith, the dispersion coefficient was $V_{e1} = 47.40$ %. This value was addopted as the solicitation dispersion for the 112 frame, that is,

ISSN 2176-5480

$$V_S(112) = 47.40\% \, . \tag{19}$$

Again, considering the reliability level of 99 % in the hoop and the respective values of z and z_5 and appying these values in equations (16), (17) e (15), results the design factor $n = 2.57$ for the 112 frame, that is,

$$n(112) \cong 2.6 \, . \tag{20}$$

Table 4 presents the necessary data calculated for both the frames.

Table 4. Results summary for 132 and 112 frames.

Carcaça	C [%]	z	z_5	V_S [%]	V_R [%]	δ_S	δ_R	n
132	99	2.326	2.700	65.73	13.06	-2.1496	0.8757	3.1
112	99	2.326	2.700	47.40	13.06	-0.6379	0.8757	2.6

These results show that the stresses dispersion generated in the 112 frame is 28 % lower than the dispersion of the stresses generated in the 132 frame. This redution follows the redution of the assembly interference between these two frames. This is because the 112 frame is stiffer than the 132 frame, which has bigger inner diameter. The higher stiffness minimize form errors and so, the interference dispersions.

Notice that the standard frames, from which this new line was derived, don't present any history of rupture of its bodys during the insertion process. Because of that, it was necessary to evaluate only the hoop region, since this is the region which was modified by tooling, so, more susceptible to rupture.

6. RESULTS AND ANALYSIS

Once validated, the finite element model was used to verify proposed frames, seeking for safety factors succevely higher. The criterion for approval was that the minimum safety factor obtained anyplace in the hoop must be higher or at least equal to the design factor calculated for this frame. In the proposal definition, it was used as reference the hatched face shown in Fig. 6. This face served as reference to define the tooling depth. The tooling depth is defined from the the hatched face towards to the frame center. Thus, the face is considerated as the zero quote and a tooling with depth of 5 mm, as an example, presents a tooling of 5 mm from the face towards to the frame center. Table 5 presents all the evaluated proposals. They are numbered from 0 to 3, being the proposal 3 considered approved. To exemplify the utilization of the face as reference, take as an example the abbreviation TF15. This means Tested Frame with a 15 mm tooling depth from the hatched face towards the frame center. In the same way, the proposal PF0 means Proposed Frame with a 0 mm tooling depth from the hatched face towards the frame center, that is, a tooling tangent to the face.

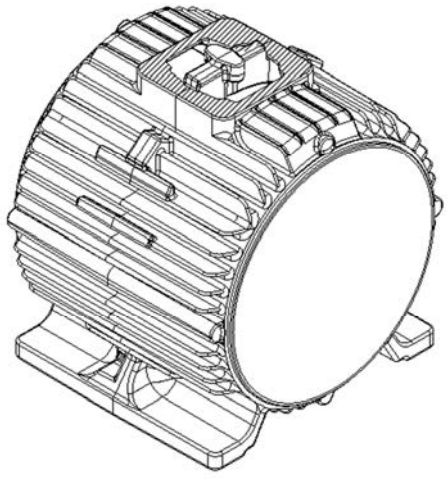

Figure 6. The hatched face was used as reference in the results evaluation.

Looking at Tab. 5 one can see that in the manner that the tooling depth becomes lower, the corresponding safety factor becomes higher. This hapens mainly for the 132 frame. For the 112 frame, the safety factor stabilizes in 1.6 when the tooling depth is 5 mm or less, as can be see in the proposals 1 and 2 in Tab. 5. The minimum tooling depth required

ISSN 2176-5480

for making possible to accommodate the motor cables without damage is the tooling tangent to the face, or a 0 mm tooling depth. This is represented by the proposals 2 for both the frames. Note that in this configuration, the higher safety factors obtained were 1.4 for the 132 frame and 1.6 for the 112 frame. As it is not possible to alter any other geometric configuration in the frame, the only manner to improve the safety factor was to modify the frame inner diameter tooling tolerance. After some tests, it was verified that using the tolerance of + 0.07 mm to + 0.10 mm, it was possible to obtain the desired safety factors, which are 3.1 for the 132 frame and 2.6 for the 112 frame. They have the same values of the calculated design factors, so this is enough for approval.

Looking the dispersion coefficients presented in Tabs. 1 and 4, along with the respective calculated design factors, it is possible to conclude that the dispersion coefficient and consequently the design factor are higher for the 132 frame than to the 112 frame. The 132 frame has bigger size, and consequently the lower stiffness. So, it is expected that in the manner that the frame size (or its inner diameter) is smaller, its sttiffness is higher and consequently the dispersion coefficient will be lower, resulting in design factors always lower than the one calculated for the 132 frame, which is the biggest frame from this product line. Herewith, as a praticum guide, the design factor of 3.1, calculated form the 132 frame could be adopted for the other frames, which have inner diameters successively smaller than the 132 frame. This is very important for the industry, since it represents costs redution in tests, instrumentation and time analysis.

Table 5. Obtained results for the 132 and 112 frames.

132 IEC Frame				
Dimension [mm]		$219.9\ ^{+0.07}_{+0.00}$		
Configuration	0	1	2	3
Description	TF15	PF5	PF0	PF0T
Safety factor	1.1	1.3	1.4	3.1
112 IEC Frame				
Dimension [mm]		$181.9\ ^{+0.07}_{+0.00}$		
Configuration	0	1	2	3
Description	TF7	PF5	PF0	PF0T
Safety factor	1.3	1.6	1.6	2.6

Legend:
TF7/15 = **T**ested **f**rame with tooling of 7 and 15 mm beyond the face, respectively.
PF5/0/0T = **P**roposed **f**rame with tooling of 5 and 0 mm beyond the face and 0 mm beyond the face with change in the tolerance value, respectively.

7. CONCLUSIONS

This work can be splitted in three very distinct parts, but complementary to each other. The experimental part; the validation of the finite element model part with the experimental results; and the probabilistic part. Roughly, the validation of the finite element model part demanded around 40 % of the total time. The other 60 % were equaly divided between the experimental and probabilistic parts.

The validation was crucial for the continuity of the work and it was possible because of the strains measured by the strain gages attached directly to the frames during the insertion process of the stator into the frame. Only after the validation it was possible to evaluate the proposals for the frame.

Another point was the statistical treatment given to the material resistance and solicitation data. The last represented by the probabilistic distribution of the stresses resulting in the hoop as function of the interference linkage between stator and frame. This treatment leads to the design factor determination, which is a probabilistic safety factor for the component. It takes into account also the confidence level desired for the component, being this an entry data. The design factor calculation eliminates common questions like: Which is the adequate safety factor for the design? This doubth always emerges in the deterministic designs which are usually done in the industry and when the addoption of one or other values for the safety factor may lead to an extremelly oversized structure, wasting money, or to an undersized structure, putting in risk the integrity and the life as whole.

The major difficult in applying the structural reliability theory for the determination of a design factor for the system is that the deep knowledge of the material used in producing the components as well as the solicitation demanding the system are critical. Besides, the solicitations are not summarized by the loads applied on the components, but by the geometric deviations coming from the production process. The bondary conditions also plays an important role in this scenary and must be checked with caution in each case.

ISSN 2176-5480

8. ACKNOWLEDGMENTS

The authors are thankful to WEG Electric Equipments S.A. for supporting the prototypes and tests.

9. REFERENCES

Ansys Reference Manual Release 14.0.

Associação Brasileira de Normas Técnicas, 1986. “NBR 6589: Peças em ferro fundido cinzento classificadas conforme a resistência à tração”, Brasil, 11 p.

Beck, R.; Campregher, M.A., 2012, “Análise experimental de tensões por meio de extensômetros elétricos de resistência”, WEG Electric Equipments S.A., Jaraguá do Sul, Brazil.

Benjamin, J.R.; Cornell, C.A., 1970, “Probability, statistics and decision for civil engineers”, McGraw-Hill, Inc., New York, USA.

Dally, J.M; Riley, W.F., 1991, “Experimental stress analysis”, McGraw-Hill, Inc., New York, USA.

Grante - Grupo de Análise e Projeto Mecânico, July 2004, “Extensometria: UFSC Course” (in portuguese), Mechanical Engineering Department, Federal University of Santa Catarina, Brazil, Course notes, 47 p.

Hugues, T.J.R., 1987, “The finite element method”, Prentive-Hall Inc., New Jersey, USA.

Kececioglu, D.; Lamarre, G., 1978, “Designing mechanical components to a specified reliability and confidence level”, Nuclear Engineering and Design, Vol.50, pp. 149-162.

Kester, W., 1999, “Practical design techniques for sensor signal conditioning”, Analog Devices, Inc., Norwood, Massachusetts, USA.

Knapp, J.; *et al*., 1998, “Measurement os shock events by means of strain gauges and accelerometers”, Elsevier Measurement Jornal, Vol.24, pp. 87-96.

Shigley, J.E., 1984, “Elementos de máquinas 2”, Editora LTC S.A., Rio de Janeiro, Brasil.

Shigley, J.E.; Mischke, C.R.; Budynas, R.G., 2005, “Projeto de engenharia mecânica”, Bookman, Porto Alegre, Brasil.

Simo, J.C. and Hugues, T.J.R., 1998, “Computational inelasticity”, Springer-Verlag Inc., New York, USA.

10. RESPONSIBILITY NOTICE

The authors are the only responsible for the printed material included in this paper.